CuPt ordering in high bandgap $Ga_xIn_{1-x}P$ alloys on relaxed GaAsP step grades

M. A. Steiner,[1,a] L. Bhusal,[1] J. F. Geisz,[1] A. G. Norman,[1] M. J. Romero,[1] W. J. Olavarria,[1] Y. Zhang,[2] and A. Mascarenhas[1]
[1]*National Renewable Energy Laboratory, Golden, Colorado 80401, USA*
[2]*Department of Electrical and Computer Engineering, University of North Carolina at Charlotte, Charlotte, North Carolina 28223, USA*

(Received 6 July 2009; accepted 5 August 2009; published online 24 September 2009)

We have fabricated a series of $Ga_xIn_{1-x}P$ samples over the compositional range $0.51<x<0.76$ on GaAs substrates. The samples were prepared by first growing a thick step-graded layer of $GaAs_{1-y}P_y$ to bridge the lattice misfit between the $Ga_xIn_{1-x}P$ layers and the GaAs substrate. The order parameter was tuned using a dilute antimony surfactant during growth. The composition, strain, and order parameter of each sample were characterized by x-ray diffraction, and the bandgap was measured by photoluminescence. We find good agreement between the experimentally measured bandgaps and theoretically modeled curves. © *2009 American Institute of Physics*. [doi:10.1063/1.3213376]

I. INTRODUCTION

$Ga_xIn_{1-x}P$ has been studied extensively for many years and is an important technological material for the photovoltaics industry. Lattice-matched to GaAs ($x=0.516$) or Ge ($x=0.505$), the alloy forms the top subcell in high-efficiency multijunction solar cells, in which conversion efficiencies of 40.8% and 40.1% have recently been demonstrated.[1,2] At room temperature, the GaAs-matched alloy exhibits a bandgap as high as 1.91 eV,[3] but significant improvements in the performance of multijunction solar cells may call for a top subcell with a higher bandgap in the 2.0–2.1 eV range.[4] With sufficient material quality, higher bandgap alloys could also be suitable for the development of very high efficiency light-emitting diodes (LEDs) for solid state white-light applications, filling the red emission (~615–625 nm) and the green emission (~540–570 nm) gaps.[5,6]

It is well established that under certain growth conditions GaInP exhibits a tendency toward kinetic ordering, which has a strong influence on the bandgap. In particular, epilayers grown by metalorganic vapor phase epitaxy (MOVPE) tend to exhibit a partially ordered CuPt crystal structure,[7,8] leading to a reduction in the bandgap of >100 meV.[9,10] Experimental work on ordering has been largely confined to the lattice-matched alloy, however, with a few notable exceptions. Using electron diffraction, Kondow *et al.*[11] observed CuPt ordering in a $Ga_{0.7}In_{0.3}P$ alloy, and Lin *et al.*[12] observed similar ordering in a $Ga_{0.65}In_{0.35}P$ alloy. Both of these studies looked at epilayers that were lattice-matched to commercially available substrates of GaAsP/GaAs. Yuan *et al.*[13] investigated the growth and characterization of $Ga_xIn_{1-x}P$ with $x=\{0.51,0.65,0.69\}$ for LED applications, but no ordering was discussed. Mori and Fitzgerald[14] reported an extensive study of the morphology of disordered $Ga_xIn_{1-x}P$ that was grown on a GaAsP graded layer, with x ranging from 0.6–0.8, and showed that a growth temperature of 725 °C instead of 650 °C could effectively disorder the alloy and raise the bandgap. They also showed data on the effect of disordering with an antimony (Sb) surfactant, though with a high concentration that they suggest led to Sb incorporation.

Recently, theoretical work by Zhang and co-workers,[6,15,16] based on the supercell approach to modeling the random and ordered alloys, has led to predictions for the bandgap of $Ga_xIn_{1-x}P$ across the compositional range $0<x<1$. The ordered $Ga_xIn_{1-x}P$ alloy is a $\langle 111\rangle$ monolayer superlattice of $Ga_{x+\eta/2}In_{1-(x+\eta/2)}P/Ga_{x-\eta/2}In_{1-(x-\eta/2)}P$, where the order parameter η has a maximum value of $\eta_{max}(x)=\min[2x,2(1-x)]$. At $x=0.5$, the fully ordered structure is a superlattice of alternating $\{1\bar{1}1\}$ or $\{\bar{1}11\}$ monolayers of GaP and InP. Depending on the substrate miscut, one or both variants may be present; a GaInP epilayer grown on a GaAs substrate miscut 6° toward a $\langle 111\rangle_B$ direction can have a large uniform domain size, on the order of 1 μm, in a single $CuPt_B$ ordered variant.[17] For $x>0.5$ or $x<0.5$, the fully ordered structure becomes a pure GaP or InP monolayer alternating with a $Ga_{x'}In_{1-x'}P$ monolayer with $x'=(2x-1)$ or $2x$. In the GaAs-matched alloy, the bandgap reduction has been understood to result predominantly from the repulsion between the folded L point and the Γ point of the conduction band,[9] with a relatively small effect on the valence band.[18] More general understanding was given by Zhang *et al.*[16] for alloys across the compositional range, and the bandgap $E_g(x)$ was predicted for the cases where $\eta=0$ (disordered), $\eta=\eta_{max}(x)$, and $\eta=\frac{1}{2}\eta_{max}(x)$.

In this paper, we report on an experimental study of the interplay between the alloy composition and the degree of ordering in higher bandgap alloys $x=\{0.63,0.67,0.71,0.74,0.76\}$. We measured the composition, bandgap, and order parameter independently. We find that the order parameter can be tuned from $\eta=0$ (disordered) to $\sim\frac{1}{2}\eta_{max}(x)$ at any intermediate composition, and find reasonable agreement with the theoretical predictions. Because the lattice constants of the target alloys are several percent smaller than the lattice constant of GaAs, all of our samples

[a]Electronic mail: myles.steiner@nrel.gov.

were prepared by first growing a $GaAs_{1-y}P_y$ step-graded layer to bridge the misfit. In this way, the dislocation density is minimized and the GaInP epilayer grown is of relevance for practical GaAs-based device applications.

II. GROWTH

All samples in this work were grown by atmospheric pressure MOVPE in a custom-built vertical reactor. We used trimethylgallium, trimethylindium, arsine, and phospine as precursors for the reactants. (001) GaAs substrates, miscut 6°B toward $[1\bar{1}1]$, were mounted on a graphite susceptor and heated inductively to a growth temperature of 750 °C in a purified hydrogen atmosphere, and compositionally graded layers of $GaAs_{1-y}P_y$ were deposited at 8 μm/h. The reactor was then cooled to 700 °C under an overpressure of arsine and phosphine and the GaInP layer was deposited at 4 μm/h. The temperature was measured by a thermocouple embedded in the susceptor. The V/III ratio was maintained at 30–50 for the graded layers and 100 for the GaInP layer. The GaAsP steps were each 1 μm thick and were designed to keep the lattice misfit per step below 0.2%, which generally corresponded to a change of ~4% phosphorus per step. At this grade-rate, the step-graded layers were found to be almost completely relaxed and the epilayers exhibited very few cracks, which is critical for device performance. The grade was redesigned for each GaInP sample based on the target relaxed lattice constant of the film, with the number of steps ranging from five to ten. The GaInP layer was grown 2 μm thick. An antimony surfactant, derived from a triethylantimony (TESb) precursor, was used to disorder the GaInP during growth[19,20] by flowing at a concentration of $[Sb]/[V] \sim (1-30) \times 10^{-5}$, where $[V]$ represents the total group V vapor concentration. All of the growths began with the deposition of a 100 nm GaAs seed layer to bury any residual surface contamination.

III. MEASUREMENTS

The composition and strain of each GaInP epilayer were measured by glancing-exit reciprocal space mapping (RSM) of the {224} planes on a Bede high resolution x-ray diffractometer. The instrument used Cu $K\alpha_1$ radiation ($\lambda = 1.540\,41$ Å) with a (111) Ge monochromator, and two 0.5 mm slits in front of the detector to achieve the necessary angular resolution. This technique also allowed us to calibrate the composition of the graded layers. An example RSM is shown in Fig. 1 for a $Ga_{0.71}In_{0.29}P$ sample. The first eight layers in the grade are distinguishable, and the GaInP epilayer is seen to be coincident with the final layer in the grade. The large peak is dominated by the properties of the thick GaInP epilayer. We found the $Ga_xIn_{1-x}P$ compositions x to be within 0.005 of the nominal composition and the residual strain in the epilayers to be ≤0.15%. We did not observe any strong systematic variation in the strain as a function of composition.

The material quality was evaluated by room temperature cathodoluminescence, using a Jeol 5800 scanning electron microscope and a Roper Scientific Silicon EEV cryogenic charge coupled device (CCD). The beam energy was 15 keV

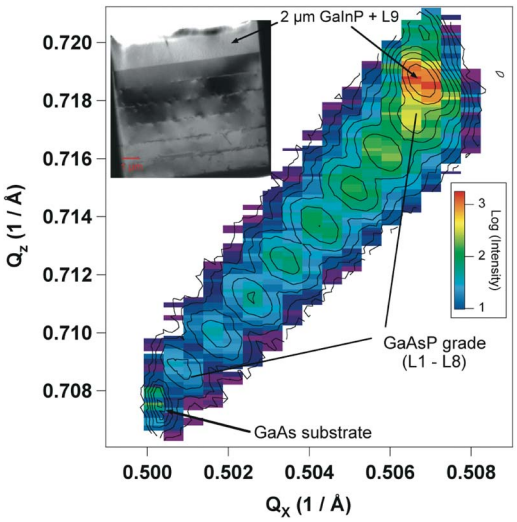

FIG. 1. (Color online) Reciprocal space map of the (224) plane of a $Ga_{0.71}In_{0.29}P$ sample, taken in glancing-exit mode. The as-grown structure has nine layers in the GaAsP grade and a final, thick layer of GaInP. The inset shows a low-magnification cross-sectional TEM image of the GaAsP layers 4–9 and the GaInP epilayer.

and the beam current was 1 nA. We found the defect density of most samples to be in the range $(3-6) \times 10^6$ cm^{-2}; one of the 76% Ga samples had a defect density of 10^7 cm^{-2}. The defect density generally increased (very weakly) with the gallium mole fraction, as might be expected given the increase in lattice misfit with respect to the substrate, but at any particular composition there was no correlation between the defect density and the order parameter. This level of defect density is good, but lower defect densities are desirable and might be achievable with improvements in the graded-layer designs.[14]

CuPt ordering was observed by transmission electron diffraction using an FEI Tecnai $G^2$30 transmission electron microscope (TEM) at an accelerating voltage of 300 kV. Figure 2 shows a [110]-pole diffraction pattern for a selected area of a $Ga_{0.71}In_{0.29}P$ epilayer. The large spots represent the

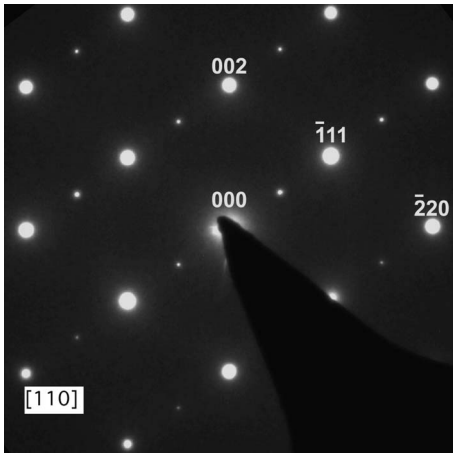

FIG. 2. [110]-pole transmission electron diffraction pattern for a $Ga_{0.71}In_{0.29}P$ sample with $\eta = 0.30 \pm 0.02$ ($\eta_{rel} = 0.54$). The larger points represent fundamental reflections as indicated. The smaller points represent the superlattice reflections for the $[\bar{1}11]$ $CuPt_B$ variant. No superlattice reflections are visible from the $[1\bar{1}1]$ variant.

fundamental reflections and small spots the superlattice reflections. There is clearly a single $CuPt_B$ variant present. Images of the orthogonal $[1\bar{1}0]$-pole do not show any superlattice reflections, indicating that there is no $CuPt_A$ ordering.

The order parameter was measured by x-ray diffraction and calculated from the ratio of the integrated intensities of the $(1\bar{1}3)$ and $\frac{1}{2}(1\bar{1}3)$ rocking curves.[21] Skew-symmetric reflections were accessed by rotating the χ-circle to 31.24° (6° miscut+25.24° surface angle), so that the incident and diffracted path lengths within the sample were approximately equal, which simplified the analysis. The rocking curves were measured with both detector slits removed.

The order parameter measurement depends on the intensities of the peaks rather than simply the positions, and accurate measurement is complicated by the presence of the GaAsP graded layer. By design, the lattice constant of the GaInP epilayer closely matches the lattice constant of the top layer in the grade, and both layers will contribute to the $(1\bar{1}3)$ reflection so that the integrated intensity will be overestimated. The GaAsP layer does not show ordering, however, so that the $\frac{1}{2}(1\bar{1}3)$ reflection will be unaffected by the graded layer. Determining the intensity of the $(1\bar{1}3)$ reflection by fitting the combined peak is difficult and inaccurate because of the nearly total overlap of the individual peaks. It is possible to measure the order parameter by comparing reflections such as the $1/2(\bar{3}33)$ and the $1/2(\bar{5}55)$,[22] but these peaks are broad and difficult to fit, and this method requires higher x-ray intensity than was available. We therefore prepared samples for these measurements by bonding the GaInP surface to a glass slide with a rigid, transparent epoxy and etching away the GaAs substrate and the GaAsP graded layers. That the grade was fully removed was verified by measuring the transmission through the now-transparent sample and observing a sharp drop only at the GaInP bandgap, as measured by photoluminescence (PL) (described below).

As described in Ref. 21, the integrated intensities were corrected for Lorentz polarization and absorption effects,[23] and for differences in structure factors. The atomic form factors were obtained from Ref. 23 and corrected for dispersion and thermal vibration using the Debye–Waller model. The Debye temperatures for GaP and InP were taken to be 495 and 422 K, respectively,[24] and all correction factors were interpolated to the specific compositions of the films. Figure 3 shows an example of the rocking curve measurements for a $Ga_{0.76}In_{0.24}P$ film. The $\frac{1}{2}(1\bar{1}3)$ reflection has much lower intensity than the fundamental $(1\bar{1}3)$ reflection, and the x-rays were collected for a longer period of time at each point. The peaks were fit to a Voigt model and the integrated intensity calculated from the fit. We were able to measure η with relative uncertainties of $\leq 10\%$.

Figure 4(a) shows how the order parameter varies with the antimony concentration for several compositions. The ratio $[Sb]/[V]$ was determined from the mass flow rates of the TESb and phosphine reactants. With no surfactant, the order parameter is determined by other growth parameters such as temperature and rate,[25] and is typically in the range of $\eta=0$

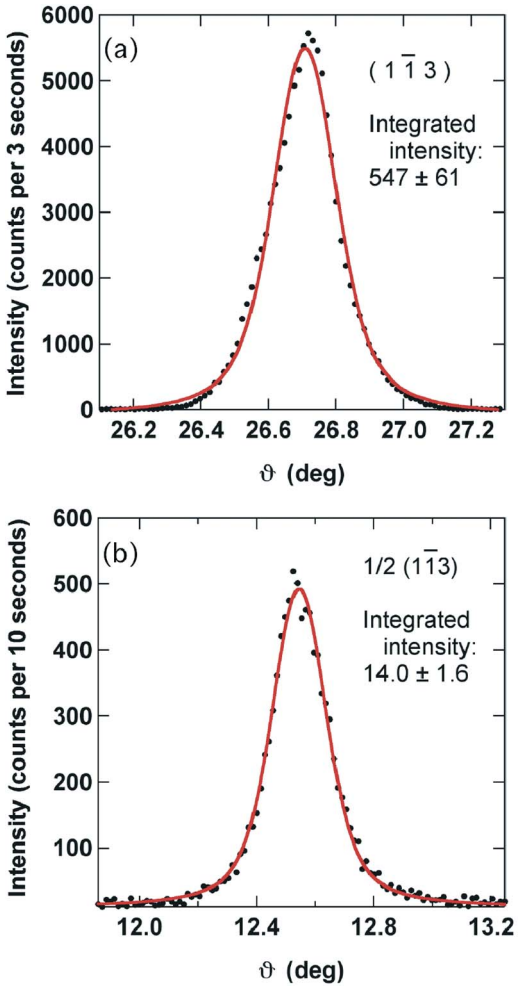

FIG. 3. (Color online) X-ray rocking curves from a $Ga_{0.76}In_{0.24}P$ film, showing (a) the fundamental $(1\bar{1}3)$ reflection, and (b) the $\frac{1}{2}(1\bar{1}3)$ superlattice reflection. Points are the data and solid lines are the Voigt fit. The order parameter for this sample was 0.22 ± 0.02.

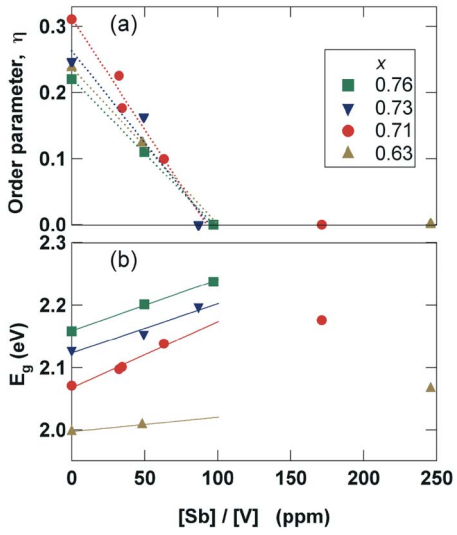

FIG. 4. (Color online) Variation in (a) the order parameter as determined from x-ray and (b) the bandgap as determined from the PL peak, with Sb concentration, at different compositions as indicated. The solid lines are linear regression fits over the limited range of [Sb]/[V] for which $\eta \geq 0$.

to $\eta \approx (1/2)\,\eta_{\max}(x)$. The effect of the surfactant is to linearly suppress the ordering, as was found for the GaAs-matched alloy.[20]

The bandgap of each sample was measured by room temperature PL using a 405 nm GaN laser to excite the sample, and a 0.27 m spectrometer followed by an air-cooled Si-CCD detector. The peak position was shifted by $-1/2k_BT$ to correct for temperature and by +5 meV to correct for the residual tensile strain.[26] As shown in Fig. 4(b), the bandgap increases linearly with the surfactant concentration over the range where the order parameter $\eta \geq 0$. The data for $x = 0.71$ indicate that the bandgap saturates at higher Sb concentrations, which is what we would expect so long as the concentration is not so high as to cause significant Sb incorporation.[14] The bandgap of the $x=0.63$ sample at $[\mathrm{Sb}]/[V] \sim 250$ ppm is higher than expected, though the scarcity of data at lower Sb concentrations precludes an accurate fit in that range.

IV. DISCUSSION

Figure 5(a) shows PL measurements for a set of $Ga_{0.76}In_{0.24}P$ films with varying degrees of order. The asymmetric lineshape for the ordered samples is likely due to the carrier thermalization into the second valence band because ordering also splits the Γ_8-like valence band.[6] The most ordered sample, with $\eta=0.22$, shows a bandgap reduction of $\Delta E=-79$ meV relative to the fully disordered sample. As argued in Ref. 9, the CuPt ordering causes the L-point along the ordering direction to fold into the Γ-point, which results in a coupling of the original bands and a repulsion between the conduction band minimum and the L-point, and therefore a reduction in the bandgap. The magnitude of the repulsion is influenced by the degree of ordering and by the proximity to the Γ-X (direct-indirect) crossover. Note that the PL intensity increases whereas the linewidth decreases with increasing order parameter. The intensity increase is primarily due to the reduction in thermalization loss as a result of the lowering of the Γ-like bandedge, while the linewidth decrease could be the result of the reduction in alloy scattering. The inset shows the linear variation in the bandgap with η for two different compositions, which confirms the theoretical prediction[27] for the nonanalytic η dependence near the direct-indirect crossing point at $x \sim 0.75$. Figure 5(b) shows PL for a series of partially ordered films $[\eta_{\mathrm{rel}} = \eta/\eta_{\max}(x) \sim 0.5]$ of varying compositions, where the bandgap shift results from a Γ-L band interaction that now depends on both the composition and the degree of ordering. Because these compositions are close to the Γ-X and Γ-L crossovers, the disordering effect has a strong influence on the transition matrix element and the lowest energy Γ-like bandgap transition is only quasidirect.[6] In addition, the thermalization to nearby alloy states also quenches the bandedge PL. The PL intensity is therefore found to decrease as the bandgap increases. There is no apparent correlation between either the PL intensity or the linewidth and the defect density, indicating that the trend in PL intensity is not strongly related to material quality.

We have plotted all of our data in Fig. 6, which shows

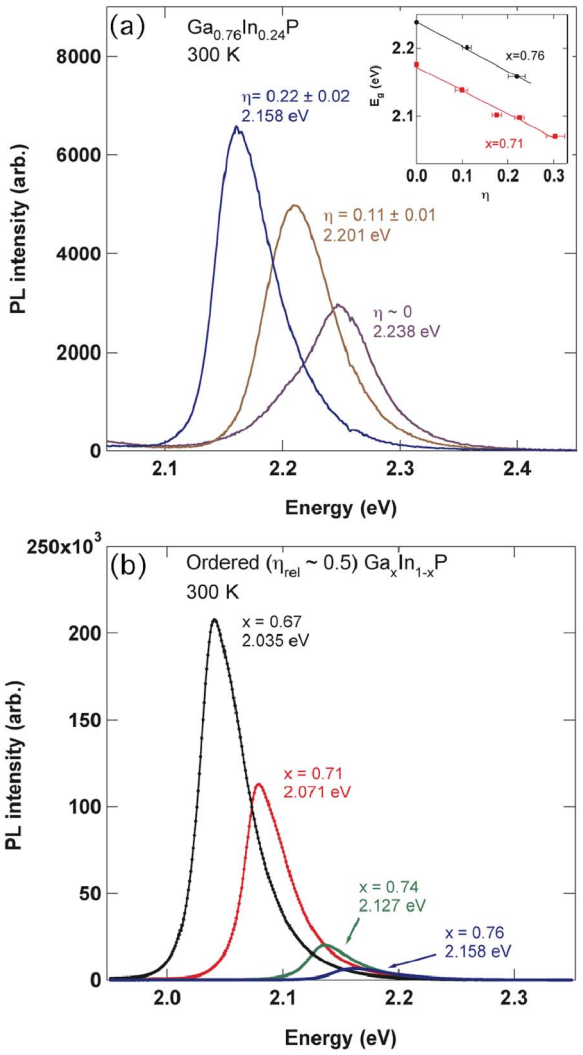

FIG. 5. (Color online) Room temperature PL measurements. (a) $Ga_{0.76}In_{0.24}P$ with different degrees of order. The inset shows the explicit variation in E_g with η for $x=0.71$ and 0.76. (b) Partially ordered ($\eta_{\mathrm{rel}} \sim 0.5$) $Ga_xIn_{1-x}P$ epilayers of different compositions. All data shown were taken on the same day so that the intensities could be easily compared.

how the bandgap $E_g(x,\eta)$ of the GaInP alloy system varies with the composition and the order parameter. The experimental points show the measured bandgaps, color-coded by the relative order parameter. Also shown are the calculated curves following Refs. 6 and 16 for the bandgaps of the disordered, half-ordered, and fully ordered alloys. The calculations were originally done at 0 K and then shifted to room temperature.[16] The measured data with $\eta_{\mathrm{rel}} \sim 0$ (purple points) and $\eta_{\mathrm{rel}} \sim 0.50 \pm 0.05$ (orange and red points) fall along the predicted curves. The green points with $\eta_{\mathrm{rel}} \sim 0.30 \pm 0.03$ have bandgaps consistent with the calculated trend. For the 1.79 eV data point at $x=0.51$, we measured an anomalously low order parameter of $\eta=0.25$ instead of the expected $\eta \sim 0.50$, but overall the experimental data are in good agreement with the calculated curves over the measurement range. We plan to extend our study to higher, indirect compositions in the future, and more carefully probe the dynamics of the direct-indirect crossover with lifetime measurements.

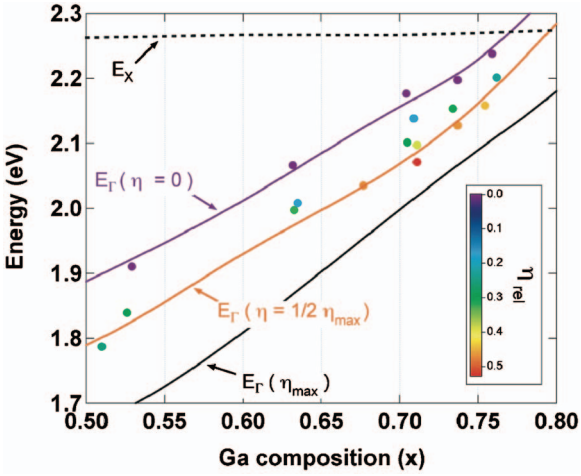

FIG. 6. (Color) Bandgap energy of the $Ga_xIn_{1-x}P$ alloy as a function of composition x and order parameter η at room temperature. Symbols are the experimental data points and are colored by relative order parameter η_{rel} as indicated by the scalebar. The purple, orange, and black lines show the Γ-like bandgap predictions for $\eta_{rel}=0$, 0.5 and 1, respectively, as described in Refs. 6 and 16. The dashed black curve is the theoretical X-point bandgap.

V. CONCLUSION

We have demonstrated the ability to control the order parameter of $Ga_xIn_{1-x}P$ from $\eta=0$ (disordered) to $\eta \sim \frac{1}{2}\eta_{max}(x)$, over the range of compositions $0.51 < x < 0.76$, by varying the concentration of a dilute Sb surfactant. Achieving an order parameter much greater than $\frac{1}{2}\eta_{max}(x)$ is very difficult under any growth condition, even in the GaAs-matched alloy. The bandgaps of the alloy system are found to be in good agreement with theoretical predictions. With increasing attention directed toward lattice-mismatched structures grown on graded layers, we anticipate that the interplay between ordering and alloying could be exploited in optoelectronic devices.

ACKNOWLEDGMENTS

It is a pleasure to thank M. Wanlass, J. Carapella, and R. Forrest for useful conversations, and K. Jones for assistance in preparing the TEM samples. This work was supported by the U.S. Department of Energy, including the Office of Energy Efficiency and Renewable Energy and the Office of Basic Science, under Contract No. DE-AC36-08GO28308 with the National Renewable Energy Laboratory.

[1] J. F. Geisz, D. J. Friedman, J. S. Ward, A. Duda, W. J. Olavarria, T. E. Moriarty, J. T. Kiehl, M. J. Romero, A. G. Norman, and K. M. Jones, Appl. Phys. Lett. **93**, 123505 (2008).
[2] R. R. King, D. C. Law, K. M. Edmondson, C. M. Fetzer, G. S. Kinsey, H. Yoon, R. A. Sherif, and N. H. Karam, Appl. Phys. Lett. **90**, 183516 (2007).
[3] M. C. DeLong, D. J. Mowbray, R. A. Hogg, M. S. Skolnick, J. E. Williams, K. Meehan, S. R. Kurtz, J. M. Olson, R. P. Schneider, M. C. Wu, and M. Hopkinson, Appl. Phys. Lett. **66**, 3185 (1994).
[4] I. Tobias and A. Luque, Prog. Photovoltaics **10**, 323 (2002).
[5] J. M. Phillips, M. E. Coltrin, M. H. Crawford, A. J. Fischer, M. R. Krames, R. Mueller-Mach, G. O. Mueller, Y. Ohno, L. E. S. Rohwer, J. A. Simmons, and J. Y. Tsao, Laser Photonics Rev. **1**, 307 (2007).
[6] Y. Zhang, A. Mascarenhas, and L.-W. Wang, Phys. Rev. B **90**, 235202 (2008).
[7] A. Gomyo, T. Suzuki, and S. Iijima, Phys. Rev. Lett. **60**, 2645 (1988).
[8] A. Mascarenhas, S. R. Kurtz, A. Kibbler, and J. M. Olson, Phys. Rev. Lett. **63**, 2108 (1989).
[9] S.-H. Wei and A. Zunger, Appl. Phys. Lett. **56**, 662 (1990).
[10] P. Ernst, C. Geng, F. Scholz, H. Schweizwer, Y. Zhang, and A. Mascarenhas, Appl. Phys. Lett. **67**, 2347 (1995).
[11] M. Kondow, H. Kakibayashi, T. Tanaka, and S. Minagawa, Phys. Rev. Lett. **63**, 884 (1989).
[12] J.-F. Lin, M.-C. Wu, M.-J. Jou, C.-M. Chang, C.-Y. Chen, and B.-J. Lee, J. Appl. Phys. **74**, 1781 (1993).
[13] J. S. Yuan, M. T. Tsai, C. H. Chen, R. M. Cohen, and G. B. Stringfellow, J. Appl. Phys. **60**, 1346 (1986).
[14] M. J. Mori and E. A. Fitzgerald, J. Appl. Phys. **105**, 013107 (2009).
[15] Y. Zhang, A. Mascarenhas, and L.-W. Wang, Phys. Rev. Lett. **101**, 036403 (2008).
[16] Y. Zhang, C.-S. Jiang, D. J. Friedman, J. F. Geisz, and A. Mascarenhas, Appl. Phys. Lett. **94**, 091113 (2009).
[17] P. Ernst, C. Geng, G. Hahn, F. Scholz, H. Schweizer, F. Phillipp, and A. Mascarenhas, J. Appl. Phys. **79**, 2633 (1996).
[18] Y. Zhang, A. Mascarenhas, and L.-W. Wang, Appl. Phys. Lett. **80**, 3111 (2002).
[19] J. K. Shurtleff, R. T. Lee, C. M. Fetzer, and G. B. Stringfellow, Appl. Phys. Lett. **75**, 1914 (1999).
[20] J. M. Olson, W. E. McMahon, and S. Kurtz, Proceedings of the 2006 IEEE Fourth World Conference on Photovoltaic Energy Conversion, Waikoloa, HI, May 2006 (unpublished), pp. 787–790.
[21] R. L. Forrest, T. D. Golding, S. C. Moss, Y. Zhang, J. F. Geisz, J. M. Olson, A. Mascarenhas, P. Ernst, and C. Geng, Phys. Rev. B **58**, 15355 (1998).
[22] J. H. Li, R. L. Forrest, S. C. Moss, Y. Zhang, A. Mascarenhas, and J. Bai, J. Appl. Phys. **91**, 9039 (2002).
[23] B. E. Warren, *X-ray Diffraction* (Dover, New York, 1990), pp. 189, 191, 253, 332, 366–373.
[24] S. Adachi, *Physical Properties of III-V Semiconductor Compounds* (Wiley, New York, 1992), p. 49.
[25] S. R. Kurtz, J. M. Olson, and A. Kibbler, Appl. Phys. Lett. **57**, 1922 (1990).
[26] S. L. Chuang, *Physics of Optoelectronic Devices* (Wiley, New York, 1995), pp. 440–443. The calculation is approximate and is based on tabulated elastic constants.
[27] Y. Zhang, A. Mascarenhas, S.-H. Wei, and L.-W. Wang, Phys. Rev. B **80**, 045206 (2009).